Photoinduced Transformation of $Cs_2Au_2Br_6$ into $CsPbBr_3$ Nanocrystals

Jishnudas Chakkamalayath,[1,2] Gregory V. Hartland[1,2] and Prashant V. Kamat[1,2,3*]

[1]Radiation Laboratory, [2]Department of Chemistry and Biochemistry, and [3]Department of Chemical and Biomolecular Engineering.

University of Notre Dame, Notre Dame, Indiana 46556, United States

Emails:

Jishnudas Chakkamalayath jchakkam@nd.edu

Gregory V. Hartland ghartlan@nd.edu

Prashant V. Kamat pkamat@nd.edu

Abstract

Lead-free halide double perovskites offer an environmentally friendly alternative to lead halide perovskites for designing optoelectronic solar cell devices. One simple approach to synthesize such double halide perovskite is through metal ion exchange. $CsPbBr_3$ nanocrystals undergo exchange of Pb^{2+} with Au(III) to form double perovskite $Cs_2Au_2Br_6$. When excited a majority of the charge carriers undergo quick recombination in contrast to long-lived charge carries of excited $CsPbBr_3$ nanocrystals. The metal ion exchange process can be reversed by adding excess PbI_2 to the suspension. Interestingly, when subjected to visible light irradiation, $Cs_2Au_2Br_6$ nanocrystals eject reduced Au out of the lattice as evidenced from the formation of larger size gold nanoparticles. The residual Pb2+ ions present in the suspension restores the original $CsPbBr_3$ composition. The results presented here provide insight into the dynamic nature of Au within the perovskite lattice under both chemical and light stimuli.

TOC Graphics

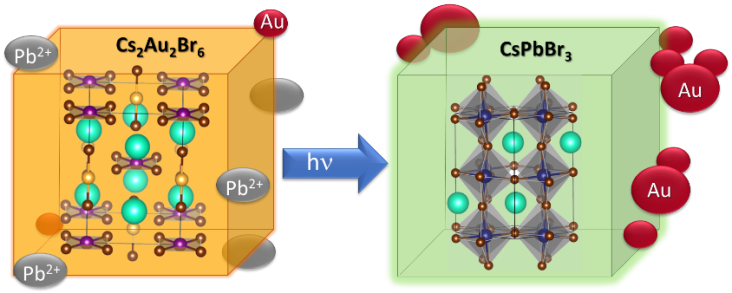

Introduction

Lead halide perovskites have drawn attention in designing as solar cells,[1-4] light-emitting diodes,[5-6] lasers[7-9] and high energy radiation detectors.[10-12] The spectral tunability and high defect tolerance have made them excellent candidates as light absorbers in optoelectronic devices. However, chemical instability and toxicity of lead remain a major challenge to employ them in practical applications.[13-14] Several studies reported improving the stability of perovskites in protic solvents but lead toxicity still remains as a major issue.[15-17] Exploration of lead-free halide perovskites necessitates replacement of Pb^{2+} cations with other metal cations.[18-19] Although Sn^{2+} is considered a replacement to Pb^{2+}, its oxidation to Sn^{4+} has hampered the advance of Sn based perovskite devices.[20-22] Lead free double perovskites of formula $A_2B_1^{+}B_2^{3+}X_6$, a functional analogue of lead halide perovskite, offer an alternative by replacing divalent Pb^{2+} with monovalent (e.g., Ag^{+}) and trivalent (e.g., Bi^{3+}) cations. By carefully tuning these metal cations one can achieve better stability and reduce the environmental impact of toxicity. Initial research was mainly focused on Cs_2AgBiX_6 (X=Cl, Br) double halide perovskites.[23-25] Although these lead-free perovskite materials are environmentally friendly, they are yet to demonstrate photovoltaic performance that is on par with lead halide perovskite. Hence the quest to explore other double halide perovskite materials continue.

$Cs_2Au_2Br_6$ with a stoichiometry similar to Cs_2AgBiX_6 (X=Cl, Br) is another double halide perovskite with a band gap onset at 1.6 eV.[26] $Cs_2Au_2Br_6$ nanocrystals show semiconducting properties and have mixed valence states for gold. Interestingly, Au exhibits mixed valency with both the monovalent and trivalent cation sites and hence can replace Pb^{2+} with charge compensation. It can be readily synthesized through cation exchange by treating $CsPbBr_3$ nanocrystal suspensions with $AuBr_3$.[27-28] The three-dimensional Au-Br framework consists of elongated octahedra with Au(III) and compressed octahedra with Au(I) sharing the corners.[29] $Cs_2Au_2X_6$ nanocrystals with a tetragonal perovskite structure has been previously studied as bulk crystals for testing their superconducting properties.[30-31] Recently the electronic properties of mixed-valence gold perovskites consisting of Au^{III} elongated octahedra and Au^{I} compressed octahedra have been explored.[32-34]

We have now elucidated the reversibility of B-site cation exchange by chemical and light stimuli in the double perovskite $Cs_2Au_2Br_6$. In the presence of excess Au^{3+} / Pb^{2+} ions, these nanoparticles can interconvert between $CsPbBr_3$ and $Cs_2Au_2Br_6$. Under visible light irradiation, Au within the double perovskite is expelled, forming $CsPbBr_3$. Factors that govern these phase changes and the photoinduced transformations occurring in these double perovskite nanocrystals are discussed. Understanding the mechanism behind reversible cation exchange and light induced changes in the $Cs_2Au_2Br_6$ nanocrystals is key to realizing their optoelectronic applications.

Results and Discussion

Formation of $Cs_2Au_2Br_6$ nanocrystals with Metal Ion Exchange. The $CsPbBr_3$ nanocrystal suspension stabilized with oleylamine/oleic acid ligands was prepared as per the literature procedure.[35] The experimental details are given in the supporting information. The addition of $AuBr_3$ to $CsPbBr_3$ nanocrystal suspension introduces interesting effects in the composition and structure of the halide perovskite. At lower concentrations (<17.5 μM $AuBr_3$ in 27 nM $CsPbBr_3$ suspension), Au(III) ions are reduced to Au^0 by oleyl amine ligands resulting in the deposition of small (1-2 nm) Au nanoparticles on the surface of $CsPbBr_3$ nanocrystals. In our previous study we have discussed the formation of such $CsPbBr_3$-Au heterostructures and their excited state dynamics.[36-37] As the concentration of $AuBr_3$ (>1 mM) in the $CsPbBr_3$ nanocrystal suspension (100 nM) is increased, Pb^{2+} ions are exchanged with Au(III) ions. The restructuring of the lattice with Au(III) and Au (I) substitution produces double perovskite nanocrystals. As shown earlier, this exchange of metal ions (Reactions 1 and 2) results in the formation of $Cs_2Au_2Br_6$ nanocrystals.[26]

$$\text{Au(III)} \xrightarrow{RNH_2,\ [R-NH_3]^+Br^-} \text{Au(I), Au}^0 \qquad (1)$$

$$2CsPbBr_3 \xrightarrow{\text{Au(III),\ Au(I)}} Cs_2Au^{I}Au^{III}Br_6 + 2Pb^{2+} \qquad (2)$$

In the present study we prepared $Cs_2Au_2Br_6$ nanocrystals by incorporating 1 mM $AuBr_3$ to a solution of 100 nM $CsPbBr_3$ nanocrystals in toluene. Figure 1A shows the absorption spectrum of as-synthesized $CsPbBr_3$ nanocrystals before and after the exchange of Pb^{2+} with Au(III)/Au(I). $Cs_2Au_2Br_6$ nanocrystals exhibit broad absorption in the visible region with no observable emission in the region. Although an earlier study indicated that $Cs_2Au_2Br_6$ nanocrystals show very weak emission at 812 nm[26] we were not able to confirm this weak emission in our spectrofluorometer.

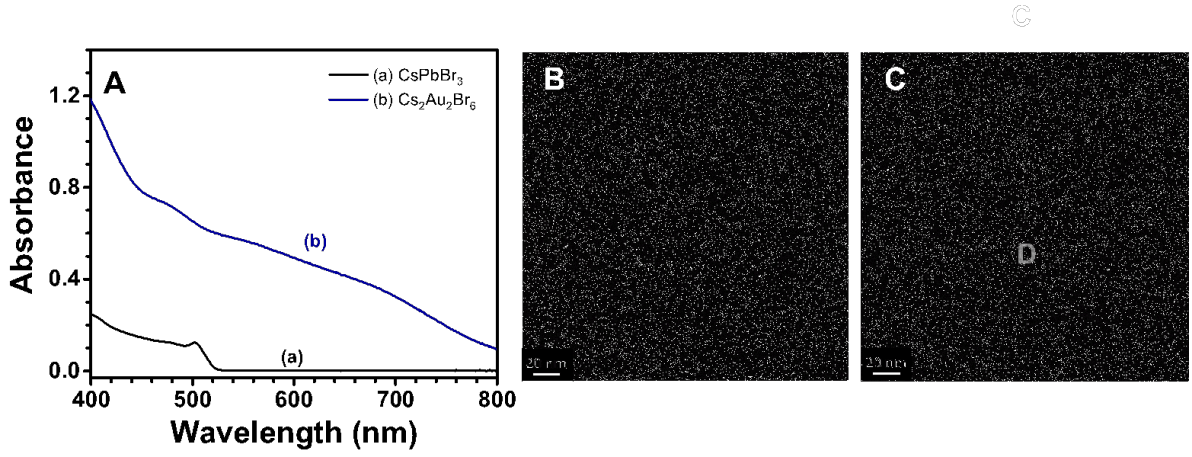

Figure 1: (A) Absorption spectra of $CsPbBr_3$ (trace a) and $Cs_2Au_2Br_6$ (trace b) nanocrystals in toluene. Representative example of TEM images of (B) $CsPbBr_3$ and (C) $Cs_2Au_2Br_6$ nanocrystals. The histogram analysis presented in SI show average size of 8.0±1.1 nm for $CsPbBr_3$ and 11.0±1.7 nm for $Cs_2Au_2Br_6$ nanocrystals.

TEM images of the $CsPbBr_3$ and $Cs_2Au_2Br_6$ nanocrystals are shown in Figures 1B and 1C. $CsPbBr_3$ nanocrystals show a cubic structure with a size distribution of 8.0±1.1 nm (See Figure S1A for size distribution analysis). Figure 1C shows the nanocrystals obtained after the exposure of 100 nM $CsPbBr_3$ nanocrystals to 1 mM $AuBr_3$ in toluene. The exchange of Pb^{2+} with Au(III)/Au(I) is also associated with the formation of Au nanoparticles. As discussed earlier[26, 36-37] the oleylamine ligands reduce the Au(III) to form nanosized gold nanoparticles. Size distribution analysis (Figure S1B) shows average sizes of 11.0±1.7 nm for $Cs_2Au_2Br_6$ nanocrystals.

The structural transformation between $CsPbBr_3$ and $Cs_2Au_2Br_6$ is shown schematically in Figure 2A. We confirmed the formation of $Cs_2Au_2Br_6$ using X-ray diffraction (XRD) analysis. The structural differences observed in powder XRD diffractograms of $CsPbBr_3$ (black trace) and $Cs_2Au_2Br_6$ (blue trace) nanocrystals are presented in Figure 2B. By comparing with previously reported structure[29] we confirm that $Cs_2Au_2Br_6$ tetragonal nanocrystals are formed as a result of metal ion exchange (Figure 2B). The peak with the asterisk in spectrum *b* (Figure 2B) corresponds to the (111) lattice plane of cubic gold. The sharp (111) cubic gold peak include contributions from the Au deposited on the surface of nanocrystals and free Au in the solution.

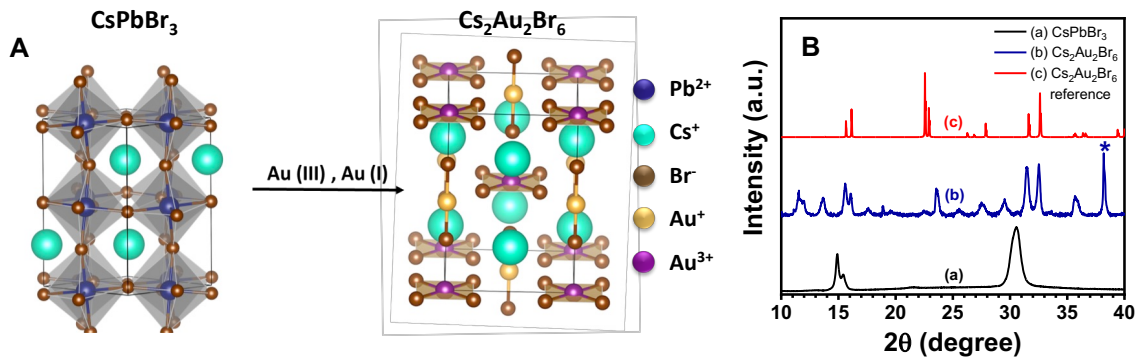

Figure 2: (A) Schematic representation showing the crystal structure of $CsPbBr_3$ and $Cs_2Au_2Br_6$ and cation exchange of Pb^{2+} and forming $Cs_2Au_2Br_6$ at high concentrations of gold. (B) Powder X-ray diffraction (XRD) diffractogram of $CsPbBr_3$ (trace a), $Cs_2Au_2Br_6$ (trace b) and $Cs_2Au_2Br_6$ reported in the literature (trace c). The asterisk denotes the peak characteristic of the (111) plane of cubic gold.

Reversibility of Metal Ion Exchange. In the previous section we discussed the preparation of $Cs_2Au_2Br_6$ nanocrystals by treating $CsPbBr_3$ nanocrystal suspension with $AuBr_3$. In order to see the reversibility of exchange between Au(III) and Pb^{2+} we exposed $Cs_2Au_2Br_6$ nanocrystal suspension to $PbBr_2$. In the presence of excess Pb^{2+}, $Cs_2Au_2Br_6$ nanocrystals were converted back to original $CsPbBr_3$ composition. (Reaction 3).

$$Cs_2Au^{I}Au^{III}Br_6 + 2Pb^{2+} \rightleftharpoons 2CsPbBr_3 + Au(III) + Au(I) \qquad (3)$$

5 mM $PbBr_2$ solution was added to a suspension of $Cs_2Au_2Br_6$ nanocrystals, to achieve its conversion back to $CsPbBr_3$ nanocrystals. The transformation was monitored using absorption and emission spectra (Figure

3). The amount of $PbBr_2$ added in this case was 5 times the original amount of $AuBr_3$ added to obtain $Cs_2Au_2Br_6$ nanocrystals.

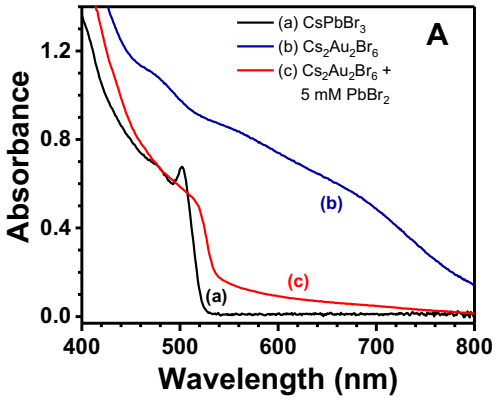

Figure 3: (A) Absorption and (B) photoluminescence ($\lambda_{excitation}$ - 375 nm) spectra of 100 nM $CsPbBr_3$ (trace a), $Cs_2Au_2Br_6$ (trace b) and $Cs_2Au_2Br_6$ with 5 mM $PbBr_2$ (trace c) nanocrystals in toluene.

Formation of $Cs_2Au_2Br_6$ nanocrystals could be tracked through the absorption and emission spectra. As $CsPbBr_3$ nanocrystal suspension was treated with $AuBr_3$, the broad absorption in the visible (Figure 3A, trace b) appears. At the same time we see quenching of emission (Figure 3B, trace b) thereby confirming the transformation of $CsPbBr_3$. When the same suspension of $Cs_2Au_2Br_6$ nanocrystals was treated with 5 mM $PbBr_2$ we see the disappearance of the broad absorption and reemergence of an exciton band closely resembling the spectral features of $CsPbBr_3$ nanocrystals. Concurrently, we also observe restoration of the green emission with emission maximum at 513 nm. The small red shift in the absorption and emission is attributed to the size increase and surface restructuring during metal ion exchange. We thus conclude that the metal ions (Pb^{2+} or Au(III)) within the perovskite structure exist in an equilibrium condition (equilibrium 3) and the perovskite composition can be modulated through the solution concentration of metal ion species.

Excited State Dynamics of $Cs_2Au_2Br_6$ nanocrystals. We employed femtosecond transient absorption

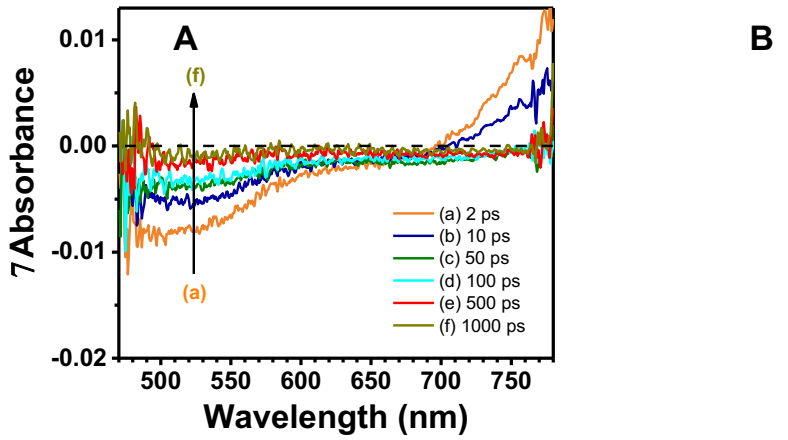

Figure 4: (A) Time-resolved transient absorption (TA) spectra recorded following laser pulse excitation (400 nm) of $Cs_2Au_2Br_6$ nanocrystals in deaerated toluene. (B) Bleach recovery (520 nm) and induced absorption (750 nm) for 75 nM $Cs_2Au_2Br_6$ nanocrystal suspension in deaerated toluene (pump wavelength - 400 nm; pump fluence – 15 μJ/cm^2).

spectroscopy to elucidate the excited state dynamics of $Cs_2Au_2Br_6$ nanocrystals in toluene. The time resolved transient absorption spectra obtained after 400 nm laser pulse excitation are shown in Figure 4A. The transient spectra recorded immediately after laser pulse excitation shows a broad bleach at wavelength below 650 nm mirroring the ground state absorption of $Cs_2Au_2Br_6$ nanocrystals. We also observe an induced absorption at wavelengths greater than 700 nm. The kinetic traces recorded at 750 nm and bleaching recovery at 520 nm are shown in Figure 4B. The induced absorption at 750 nm decreases within 30 ps. A similar fast decay component is also seen in the bleaching recovery recorded at 520 nm. However, the bleaching recovery also has a long-lived component (lifetime >200 ps). The fast component of the transient bleach recovery and decay of induced absorption reflect charge carrier relaxation within the conduction and valence bands, followed by recombination of the charge carriers. Similar excited state properties of double perovskites like Cs_2AgBiX_6 have also been noted in previous studies.[38-39] This behavior reflects the fast recombination of charge carriers as a major deactivation pathway of excited $Cs_2Au_2Br_6$ nanocrystals. This excited state behavior is distinctively different than the parent $CsPbBr_3$ nanocrystals prior to Au(III) exchange which shows long-lived charge carriers (Table S1 in the supporting information).[40]

Effect of steady state irradiation. The $Cs_2Au_2Br_6$ nanocrystals have a band gap absorption onset at 1.6 eV.[26] In order to assess the long-term photostability and to probe the photochemical transformations, $Cs_2Au_2Br_6$ nanocrystal suspension was irradiated with visible light (λ>400 nm, 100 mW/cm^2).

Figure 4A shows the absorbance spectra of $Cs_2Au_2Br_6$ nanocrystals at different steady-state irradiation

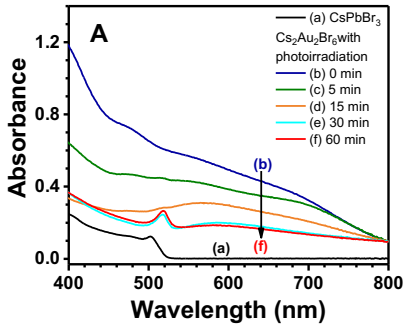

Figure 5: (A) Absorption and (B) PL spectra of $Cs_2Au_2Br_6$ nanocrystals in deaerated toluene with steady state white light irradiation (100 mW/cm^2). Trace (a) corresponds to pristine $CsPbBr_3$ sample. (C) XRD diffractogram of $CsPbBr_3$ (trace a), $Cs_2Au_2Br_6$ (blue trace) and $Cs_2Au_2Br_6$ after 60 minutes of irradiation (red trace). The asterisk denotes the peak characteristic of the (111) plane of cubic gold.

times. With increasing irradiation time, a decrease in absorbance was observed and a new peak at 517 nm appeared after 60 minutes of irradiation. We also checked the emission spectra before and after irradiation (Figure 4B). An emission band with maximum at 523 nm appeared with almost the same intensity as that of the $CsPbBr_3$. The red shift observed in the absorption and emission after irradiation can be ascribed to the changes in the morphology (Figure S1C). As a control, we kept $Cs_2Au_2Br_6$ nanocrystal suspension in dark for 2 days. No changes in the absorption features could be seen in the absence of light (Figure S2A and S2B in the supporting information) indicating the stability of $Cs_2Au_2Br_6$ in the absence of light. This observations further confirms that the spectral changes we see in Figures 5 A and B originate only during steady state irradiation.

The XRD diffractogram of $Cs_2Au_2Br_6$ after 60 minutes of visible light irradiation showed peaks similar to that of $CsPbBr_3$ nanocrystals (Figure 4C). The XRD pattern and emission recovery indicate that $Cs_2Au_2Br_6$ nanocrystals undergo photoinduced transformation to regenerate $CsPbBr_3$ nanocrystals. It should be noted the Pb^{2+} ions are present in the suspension when they were expelled from the lattice during cation exchange with $AuBr_3$. These Pb^{2+} ions were responsible in restoring $CsPbBr_3$ during steady state irradiation. The photoinduced transformation was dependent on the light intensity, and we found a threshold of 60 mW/cm^2 visible light intensity to initiate the transformation.

Mechanism of Photoinduced Expulsion of Au from $Cs_2Au_2Br_6$. As discussed in the previous section, continuous photoirradiation of $Cs_2Au_2Br_6$ causes restoration of $CsPbBr_3$ composition. The photogenerated electrons in $Cs_2Au_2Br_6$ reduce the interstitial Au(I)/Au(III). Consequently, the reduced product (Au^0) gets expelled as Pb^{2+} in solution occupies the B site to restore $CsPbBr_3$ (reactions 4 and 5).

$$Cs_2Au_2Br_6 + h\nu \longrightarrow CsPbBr_3 \text{ (e..h)} \qquad (4)$$

$Cs_2Au_2Br_6(ne) + Pb^{2+} \longrightarrow CsPbBr_3 + Au^0$ (5)

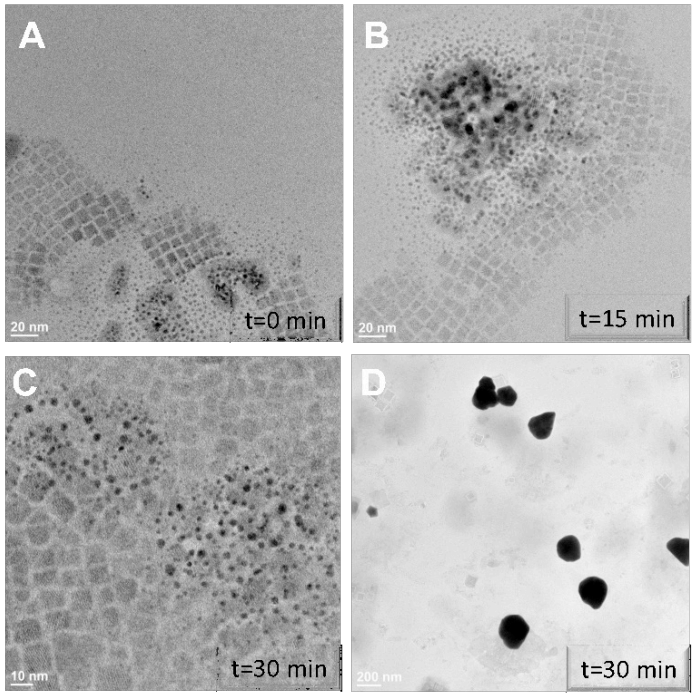

Figure 6: TEM images of $Cs_2Au_2Br_6$ nanocrystal samples following photoirradiation (white light, 100 mW/cm^2) at times, (A) 0 minutes, (B) 15 minutes, (c) 20 minutes, and (D) 30 minutes. Note that C and D are recorded at two different magnifications.

Photoirradiation is also known to alter the mixed valence state of Au(I)/Au(III) in bulk $Cs_2Au_2Br_6$, thus, bringing in instability.[31, 41-42] As the Au(III) in the lattice is reduced to form single valence phase and further reduction to for Au^0, it triggers the cation exchange with Pb^{2+} and reemergence of $CsPbBr_3$ nanocrystals.

The TEM images (Figure 6) show the morphological evolution of $Cs_2Au_2Br_6$ as the nanocrystal suspension is irradiated. The TEM image recorded before the irradiation shows $Cs_2Au_2Br_6$ nanocrystals coexisting with preformed Au nanoparticles. Following 15 min photoirradiation we observe crowding of Au nanoparticles along with growth in particle size. The TEM images recorded after 30 min of photoirradiation show $CsPbBr_3$ nanocrystals along with the appearance of larger Au nano particles. These images further confirm the light induced reduction of Au(I)/Au(III) to form Au^0 and their aggregation to form larger nanoparticles. Similar photoinduced growth of small nanoparticles to form larger Au nanoparticles has also been observed for Au-$CsPbBr_3$ heterostructures.[37] The conversion of Au(I)/Au(III) to nanoparticles prevents its direct exchange with Pb^{2+} ions. The $CsPbBr_3$ formed at the end of photoirradiation remains stable without undergoing additional cation exchange. As a result of formation of nanoparticles, the process of Pb^{2+} exchange with Au(I)/Au(III) cannot be reversed after stopping the photoirradiation for 60 minutes.

Although steady-state irradiation of $Cs_2Au_2Br_6$ induces Au expulsion, we found that femtosecond laser pulse excitation did not induce these morphological changes. This allowed us to probe changes of the excited state of $Cs_2Au_2Br_6$ during several intermediate points in Au expulsion without complications from

the laser excitation source. The time-resolved transient absorption spectra (Δt=2ps) of $Cs_2Au_2Br_6$ nanocrystals in toluene at different steady-state irradiation times were monitored (Figure 5A, see also Figures S4A-S4E in SI). The spectrum before irradiation exhibits a broad bleach below 600 nm and an induced absorption in the 700-750 nm region characteristic of $Cs_2Au_2Br_6$. As we irradiate the sample with our steady-state white light source, the bleach band became narrower, and the induced absorption disappeared. The spectrum recorded after 60 min irradiation shows a narrow bleach band similar to what we observe for $CsPbBr_3$ nanocrystals. These spectral changes further confirm the evolution of $CsPbBr_3$ nanocrystals as we continuously irradiate the $Cs_2Au_2Br_6$ nanocrystals.

The bleach recovery recorded at the bleach maximum for $CsPbBr_3$ nanocrystals (510 nm) prepared

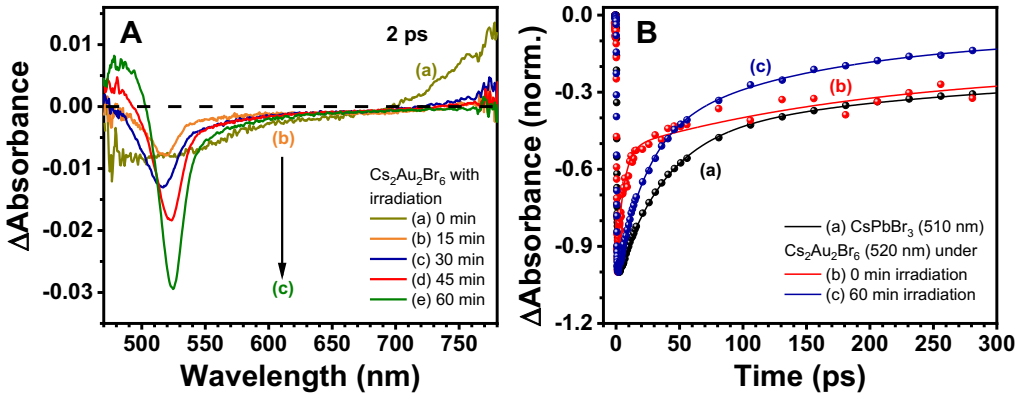

Figure 7: (A) Time-resolved transient absorption (TA) spectra recorded following laser pulse excitation (400 nm) at 2 ps of $Cs_2Au_2Br_6$ nanocrystals in toluene at different steady-state irradiation times. (B) Bleach growth and recovery recorded at bleach maximum for $CsPbBr_3$ (510 nm) and $Cs_2Au_2Br_6$ (520 nm) nanocrystals suspension at 0 minutes and 60 minutes of irradiation over 300 ps time scale (normalized to -1). Au expulsion was induced using a separate steady-state white light source (λ > 400 nm; 100 mW/cm^2).

separately are compared with the bleach recovery (520 nm) of $Cs_2Au_2Br_6$ before and after irradiation (Figure 7B). The fast time component of the bleach recovery increased from 5.3 ps to 23.1 ps as we irradiate the $Cs_2Au_2Br_6$ sample with white light (Table S2 in the supporting information). The observed trend of the bleach recovery kinetics reverting to that of pristine $CsPbBr_3$ confirms that the nanocrystal composition is restored to $CsPbBr_3$. The different recovery time can be attributed to formation of additional surface defects during the expulsion of Au and reinsertion of Pb.

We have previously shown that small Au nanoparticles can be deposited on the surface of $CsPbBr_3$, forming a metal-semiconductor heterostructure with improved charge separation.[36] However, under light irradiation the Au particles accumulate electrons and become charged, which causes the Au particles to dissociate from the nanocrystal surface entirely.[37] These previous results, along with the results presented in the current study, begin to paint a broader picture of the challenges of incorporating noble metals like Au into halide perovskites. The use of an inorganic shell around the perovskite nanocrystal (e.g. CdS[43], ZnS[44]) is one possible route to establish a stable Au-containing perovskite nanostructure.

To summarize, $Cs_2Au_2Br_6$, readily undergo cation rearrangement with visible light irradiation. The "soft lattice" structure of halide perovskites not only allows synthesis of $Cs_2Au_2Br_6$ by introduction of Au(III) ions to $CsPbBr_3$ suspension, but also reverts to $CsPbBr_3$ in the presence of Pb^{2+} ions. Visible light irradiation of $Cs_2Au_2Br_6$ suspension results in the reduction of Au(I) and Au(III) ions followed by the expulsion of Au from the host lattice. Such transformations of $Cs_2Au_2Br_6$ raise the question about their application in photocatalytic and light energy conversion devices. Efforts are underway to add a protective shell of polymer to the $Cs_2Au_2Br_6$ nanocrystal so that the expulsion of Au is suppressed.[16] Similar strategy of capping $CsPbBr_3$ nanocrystals with CdS has facilitated photocatalytic electron transfer in polar solvents.[45]

Acknowledgement

The research described herein is supported by the Division of Chemical Sciences, Geosciences, and Biosciences, Office of Basic Energy Sciences of the U.S. Department of Energy, through award (award DE-FC02- 04ER15533. GVH acknowledges support of the National Science Foundation through Grant CHE-2002300. We also acknowledge the University of Notre Dame Equipment Restoration and Renewal (ERR) program for the purchase of the Spectra Physics laser used for the transient absorption measurements. This is contribution number NDRL No. 5323 from the Notre Dame Radiation Laboratory.

Supporting Information The supporting information include control experiments, histogram analysis, emission spectra and transient absorption measurements. The Supporting Information is available free of charge at https://pubs.acs.org/doi/10.1021/XXXX

References

1. Manekkathodi, A.; Chen, B.; Kim, J.; Baek, S.-W.; Scheffel, B.; Hou, Y.; Ouellette, O.; Saidaminov, M. I.; Voznyy, O.; Madhavan, V. E., Solution-processed perovskite-colloidal quantum dot tandem solar cells for photon collection beyond 1000 nm. *Journal of Materials Chemistry A* **2019,** *7* (45), 26020-26028.
2. Chen, J.; Park, N.-G., Materials and methods for interface engineering toward stable and efficient perovskite solar cells. *ACS Energy Letters* **2020,** *5* (8), 2742-2786.
3. Li, M.; Li, H.; Fu, J.; Liang, T.; Ma, W., Recent progress on the stability of perovskite solar cells in a humid environment. *The Journal of Physical Chemistry C* **2020,** *124* (50), 27251-27266.
4. Rahmany, S.; Etgar, L., Semitransparent Perovskite Solar Cells. *ACS Energy Letters* **2020,** *5* (5), 1519-1531.
5. Wei, Y.; Cheng, Z.; Lin, J., An overview on enhancing the stability of lead halide perovskite quantum dots and their applications in phosphor-converted LEDs. *Chemical Society Reviews* **2019,** *48* (1), 310-350.
6. Wang, X.; Bao, Z.; Chang, Y.-C.; Liu, R.-S., Perovskite quantum dots for application in high color gamut backlighting display of light-emitting diodes. *ACS Energy Letters* **2020,** *5* (11), 3374-3396.
7. Zhu, H.; Fu, Y.; Meng, F.; Wu, X.; Gong, Z.; Ding, Q.; Gustafsson, M. V.; Trinh, M. T.; Jin, S.; Zhu, X., Lead halide perovskite nanowire lasers with low lasing thresholds and high quality factors. *Nature materials* **2015,** *14* (6), 636-642.

8. Veldhuis, S. A.; Boix, P. P.; Yantara, N.; Li, M.; Sum, T. C.; Mathews, N.; Mhaisalkar, S. G., Perovskite materials for light-emitting diodes and lasers. *Advanced materials* **2016,** *28* (32), 6804-6834.
9. Xu, Y.; Chen, Q.; Zhang, C.; Wang, R.; Wu, H.; Zhang, X.; Xing, G.; Yu, W. W.; Wang, X.; Zhang, Y., Two-photon-pumped perovskite semiconductor nanocrystal lasers. *Journal of the American Chemical Society* **2016,** *138* (11), 3761-3768.
10. Kasap, S.; Frey, J. B.; Belev, G.; Tousignant, O.; Mani, H.; Greenspan, J.; Laperriere, L.; Bubon, O.; Reznik, A.; DeCrescenzo, G., Amorphous and polycrystalline photoconductors for direct conversion flat panel X-ray image sensors. *Sensors* **2011,** *11* (5), 5112-5157.
11. Náfrádi, B. l.; Náfrádi, G. b.; Forró, L. s.; Horváth, E., Methylammonium lead iodide for efficient X-ray energy conversion. *The Journal of Physical Chemistry C* **2015,** *119* (45), 25204-25208.
12. Wei, H.; Huang, J., Halide lead perovskites for ionizing radiation detection. *Nature communications* **2019,** *10* (1), 1-12.
13. Babayigit, A.; Ethirajan, A.; Muller, M.; Conings, B., Toxicity of organometal halide perovskite solar cells. *Nature materials* **2016,** *15* (3), 247-251.
14. Slavney, A. H.; Smaha, R. W.; Smith, I. C.; Jaffe, A.; Umeyama, D.; Karunadasa, H. I., Chemical approaches to addressing the instability and toxicity of lead–halide perovskite absorbers. *Inorganic chemistry* **2017,** *56* (1), 46-55.
15. An, M. N.; Park, S.; Brescia, R.; Lutfullin, M.; Sinatra, L.; Bakr, O. M.; De Trizio, L.; Manna, L., Low-Temperature Molten Salts Synthesis: CsPbBr3 Nanocrystals with High Photoluminescence Emission Buried in Mesoporous SiO2. *ACS energy letters* **2021,** *6* (3), 900-907.
16. Jin, X.; Ma, K.; Chakkamalayath, J.; Morsby, J.; Gao, H., In Situ Photocatalyzed Polymerization to Stabilize Perovskite Nanocrystals in Protic Solvents. *ACS Energy Letters* **2022,** *7*, 610-616.
17. Xin, Y.; Zhao, H.; Zhang, J., Highly stable and luminescent perovskite–polymer composites from a convenient and universal strategy. *ACS applied materials & interfaces* **2018,** *10* (5), 4971-4980.
18. Giustino, F.; Snaith, H. J., Toward lead-free perovskite solar cells. *ACS Energy Letters* **2016,** *1* (6), 1233-1240.
19. Kamat, P. V.; Bisquert, J.; Buriak, J., Lead-free perovskite solar cells. *ACS Energy Letters* **2017,** *2* (4), 904-905.
20. Saparov, B.; Sun, J.-P.; Meng, W.; Xiao, Z.; Duan, H.-S.; Gunawan, O.; Shin, D.; Hill, I. G.; Yan, Y.; Mitzi, D. B., Thin-film deposition and characterization of a Sn-deficient perovskite derivative Cs2SnI6. *Chemistry of Materials* **2016,** *28* (7), 2315-2322.
21. Swarnkar, A.; Ravi, V. K.; Nag, A., Beyond colloidal cesium lead halide perovskite nanocrystals: analogous metal halides and doping. *ACS Energy Letters* **2017,** *2* (5), 1089-1098.
22. Diau, E. W.-G.; Jokar, E.; Rameez, M., Strategies to improve performance and stability for tin-based perovskite solar cells. *ACS Energy Letters* **2019,** *4* (8), 1930-1937.
23. McClure, E. T.; Ball, M. R.; Windl, W.; Woodward, P. M., Cs2AgBiX6 (X= Br, Cl): new visible light absorbing, lead-free halide perovskite semiconductors. *Chemistry of Materials* **2016,** *28* (5), 1348-1354.
24. Slavney, A. H.; Hu, T.; Lindenberg, A. M.; Karunadasa, H. I., A bismuth-halide double perovskite with long carrier recombination lifetime for photovoltaic applications. *Journal of the American chemical society* **2016,** *138* (7), 2138-2141.
25. Cho, J.; DuBose, J. T.; Kamat, P. V., Charge Injection from Excited Cs2AgBiBr6 Quantum Dots into Semiconductor Oxides. *Chemistry of Materials* **2019,** *32* (1), 510-517.
26. Roman, B. J.; Otto, J.; Galik, C.; Downing, R.; Sheldon, M., Au Exchange or Au Deposition: Dual Reaction Pathways in Au–CsPbBr3 Heterostructure Nanoparticles. *Nano letters* **2017,** *17* (9), 5561-5566.
27. Swarnkar, A.; Mir, W. J.; Nag, A., Can B-site doping or alloying improve thermal-and phase-stability of all-inorganic CsPbX3 (X= Cl, Br, I) perovskites? *ACS Energy Letters* **2018,** *3* (2), 286-289.
28. Hudait, B.; Dutta, S. K.; Bera, S.; Pradhan, N., Introducing B-Site Cations by Ion Exchange and Shape Anisotropy in CsPbBr3 Perovskite Nanostructures. *Nano Letters* **2021**.

29. Matsushita, N.; Fukuhara, F.; Kojima, N., A three-dimensional bromo-bridged mixed-valence gold (I, III) compound, Cs2AuIAuIIIBr6. *Acta Crystallographica Section E: Structure Reports Online* **2005,** *61* (6), i123-i125.
30. Kitagawa, H.; Kojima, N.; Matsushita, N.; Ban, T.; Tsujikawa, I., Studies of mixed-valence states in three-dimensional halogen-bridged gold compounds, Cs 2 Au I Au III X 6 (X= Cl, Br or I). Part 1. Synthesis, X-ray powder diffraction, and electron spin resonance studies of CsAu 0.6 Br 2.6. *Journal of the Chemical Society, Dalton Transactions* **1991,** (11), 3115-3119.
31. Kojima, N.; Hasegawa, M.; Kitagawa, H.; Kikegawa, T.; Shimomura, O., PT phase diagram and gold valence state of the perovskite-type mixed-valence compounds Cs2Au2X6 (X= Cl, Br, and I) under high pressures. *Journal of the American Chemical Society* **1994,** *116* (25), 11368-11374.
32. Bajorowicz, B.; Mikolajczyk, A.; Pinto, H. P.; Miodynska, M.; Lisowski, W.; Klimczuk, T.; Kaplan-Ashiri, I.; Kazes, M.; Oron, D.; Zaleska-Medynska, A., Integrated experimental and theoretical approach for efficient design and synthesis of gold-based double halide perovskites. *The Journal of Physical Chemistry C* **2020,** *124* (49), 26769-26779.
33. Ghosh, B.; Febriansyah, B.; Harikesh, P. C.; Koh, T. M.; Hadke, S.; Wong, L. H.; England, J.; Mhaisalkar, S. G.; Mathews, N., Direct Band Gap Mixed-Valence Organic–inorganic Gold Perovskite as Visible Light Absorbers. *Chemistry of Materials* **2020,** *32* (15), 6318-6325.
34. Roy, M.; Borkar, H.; Alam, A.; Aslam, M., Spontaneous anion-exchange synthesis of optically active mixed-valence Cs 2 Au 2 I 6 perovskites from layered CsAuCl 4 perovskites. *Chemical Communications* **2021,** *57* (12), 1478-1481.
35. Protesescu, L.; Yakunin, S.; Bodnarchuk, M. I.; Krieg, F.; Caputo, R.; Hendon, C. H.; Yang, R. X.; Walsh, A.; Kovalenko, M. V., Nanocrystals of cesium lead halide perovskites (CsPbX3, X= Cl, Br, and I): novel optoelectronic materials showing bright emission with wide color gamut. *Nano letters* **2015,** *15* (6), 3692-3696.
36. Balakrishnan, S. K.; Kamat, P. V., Au–CsPbBr3 hybrid architecture: anchoring gold nanoparticles on cubic perovskite nanocrystals. *ACS Energy Letters* **2017,** *2* (1), 88-93.
37. Chakkamalayath, J.; Hartland, G. V.; Kamat, P. V., Light Induced Processes in CsPbBr3–Au Hybrid Nanocrystals: Electron Transfer and Expulsion of Au. *The Journal of Physical Chemistry C* **2021,** *125* (32), 17881-17889.
38. Buizza, L. R.; Wright, A. D.; Longo, G.; Sansom, H. C.; Xia, C. Q.; Rosseinsky, M. J.; Johnston, M. B.; Snaith, H. J.; Herz, L. M., Charge-Carrier Mobility and Localization in Semiconducting Cu2AgBiI6 for Photovoltaic Applications. *ACS energy letters* **2021,** *6* (5), 1729-1739.
39. Wright, A. D.; Buizza, L. R.; Savill, K. J.; Longo, G.; Snaith, H. J.; Johnston, M. B.; Herz, L. M., Ultrafast Excited-State Localization in Cs2AgBiBr6 Double Perovskite. *The journal of physical chemistry letters* **2021,** *12* (13), 3352-3360.
40. Manser, J. S.; Kamat, P. V., Band filling with free charge carriers in organometal halide perovskites. *Nature Photonics* **2014,** *8* (9), 737-743.
41. Kojima, N.; Kitagawa, H., Optical investigation of the intervalence charge-transfer interactions in the three-dimensional gold mixed-valence compounds Cs 2 Au 2 X 6 (X= Cl, Br or I). *Journal of the Chemical Society, Dalton Transactions* **1994,** (3), 327-331.
42. Liu, X.; Moritomo, Y.; Ichida, M.; Nakamura, A.; Kojima, N., Photoinduced phase transition in a mixed-valence gold complex. *Physical Review B* **2000,** *61* (1), 20.
43. Kipkorir, A.; DuBose, J.; Cho, J.; Kamat, P. V., CsPbBr 3–CdS heterostructure: stabilizing perovskite nanocrystals for photocatalysis. *Chemical science* **2021,** *12* (44), 14815-14825.
44. Ravi, V. K.; Saikia, S.; Yadav, S.; Nawale, V. V.; Nag, A., CsPbBr3/ZnS core/shell type nanocrystals for enhancing luminescence lifetime and water stability. *ACS Energy Letters* **2020,** *5* (6), 1794-1796.
45. Kipkorir, A.; DuBose, J. T.; Cho, J.; Kamat, P. V., CsPbBr3–CdS Heterostructure: Stabilizing Perovskite Nanocrystals for Photocatalysis. *Chemical Science* **2021**.